Spin glasses in a field: Three and four dimensions as seen from one space dimension

Derek Larson, Helmut G. Katzgraber, M. A. Moore, and A. P. Young

Phys. Rev. B **87**, 024414 — Published 18 January 2013

DOI: 10.1103/PhysRevB.87.024414

Spin glasses in a field: Three and four dimensions as seen from one space dimension

Derek Larson,[1] Helmut G. Katzgraber,[2,3] M. A. Moore,[4] and A. P. Young[5]

[1]*Department of Physics, National Taiwan University, No. 1, Sec. 4, Roosevelt Rd., Taipei 106, Taiwan*
[2]*Department of Physics and Astronomy, Texas A&M University, College Station, Texas 77843-4242, USA*
[3]*Theoretische Physik, ETH Zurich, CH-8093 Zurich, Switzerland*
[4]*School of Physics and Astronomy, University of Manchester, Manchester M13 9PL, United Kingdom*
[5]*Department of Physics, University of California, Santa Cruz, California 95064, USA*

(Dated: January 10, 2013)

We study the existence of a line of transitions of an Ising spin glass in a magnetic field—known as the de Almeida-Thouless line—using one-dimensional power-law diluted Ising spin-glass models. We choose the power-law exponent to have values that approximately correspond to three- and four-dimensional nearest-neighbor systems and perform a detailed finite-size scaling analysis of the data for large linear system sizes, both using a new approach proposed recently [Phys. Rev. Lett. **103**, 267201 (2009)], as well as traditional approaches. Our results for the model corresponding to a three-dimensional system are consistent with there being no de Almeida-Thouless line, although the new finite-size scaling approach does not rule one out. For the model corresponding to four space dimensions, the new and traditional finite-size scaling analyses give conflicting results, indicating the need for a better understanding of finite-size scaling of spin glasses in a magnetic field.

PACS numbers: 75.50.Lk, 75.40.Mg, 05.50.+q

I. INTRODUCTION

One of the most striking predictions of the mean-field theory of Ising spin glasses, taken to be the exact solution[1] of the infinite-range Sherrington-Kirkpatrick (SK)[2] model, is the existence of a line of transitions, known as the de Almeida-Thouless[3] (AT) line in the presence of a magnetic field. This line of transitions separates a high-temperature region where the description of the model is quite simple, just involving a single order parameter, from a low-temperature region where there is "replica symmetry breaking" (RSB) in which the system has an infinite number of order parameters characterized by a function.[1]

The question of whether RSB applies to realistic short-range spin glasses remains controversial. According to the RSB picture, real spin glasses behave rather similarly to the SK model and so have an AT line. However, according to the phenomenological "droplet" picture[4–7] there is no AT line and the zero-field transition is rounded out by any nonzero magnetic field in finite-dimensional short-range systems.

It is convenient for simulations that a static property, the spin-glass susceptibility $\chi_{\rm SG}$, diverges at the transition. This quantity is the inverse of the eigenvalue of the stability matrix[3] found by de Almeida and Thouless and is given by the zero-wave-vector $k = 0$ limit of $\chi_{\rm SG}(k)$ defined in Eq. (5) below. Because $\chi_{\rm SG}$ can be computed in simulations directly,[8] one might imagine that it would be straightforward to decide if the AT line occurs in, say, a three-dimensional spin glass. However, there is still no consensus on this issue because there seem to be quite large corrections to finite-size scaling (FSS). The purpose of this paper is to investigate different methods that have been proposed to perform FSS to see if there is an AT line in three and in four space dimensions.

In fact, rather than to study short-range models,[9–16] we find it convenient to study a one-dimensional model with long-range interactions which is taken as a *proxy* for a short-range model.[17–23] The interactions of the long-range model fall off with a power σ of the distance and varying the power effectively corresponds to varying the space dimension of the corresponding short-range model. Here we study long-range models which are proxies for short-range models in three and four space dimensions.

The outline of this paper is as follows. Section II describes the model, the quantities we calculate and details of the numerical simulations. Section III describes the results, and Sec. IV gives our conclusions.

II. MODEL, OBSERVABLES & NUMERICAL DETAILS

A. Model

We study a variation of the model introduced in Ref. 21 which is given by the Hamiltonian

$$\mathcal{H} = -\sum_{i,j} \varepsilon_{ij} J_{ij} S_i S_j - \sum_i h_i S_i \; . \tag{1}$$

In Eq. (1), $S_i = \pm 1$ are Ising spins placed on a ring of length L to enforce periodic boundary conditions in a natural way.[17] The interactions J_{ij} are chosen from a Gaussian distribution with zero mean and standard deviation unity. The dilution matrix ε_{ij} takes values 0 and 1, and has the probability $p_{ij} \sim r_{ij}^{-2\sigma}$ of taking the value 1, where $r_{ij} = (L/\pi)\sin(\pi|i-j|/L)$ is the geometric distance between the spins. To prevent the probability of

placing a bond between two spins being larger than 1, a short-distance cutoff is applied and thus we take

$$p_{ij} = 1 - \exp(-\mathcal{A}/r_{ij}^{2\sigma}) \,. \tag{2}$$

The constant $\mathcal{A}$ is determined by the requirement that the *mean* coordination number, $z_{\rm av}$, takes a specified value

$$z_{\rm av} = \sum_{i=1}^{L-1} p_{iL}, \tag{3}$$

and we set $z_{\rm av} = 6$. The values of $\mathcal{A}$ are given in Table I. The site-dependent random fields h_i are chosen from a Gaussian distribution with zero mean and standard deviation H.

By tuning the exponent σ in Eq. (2) one can change the universality class of the model in Eq. (1) from the infinite-range to the short-range universality case. For $0 < \sigma \leq 1/2$ the model is in the infinite-range universality class[24,25] and, in particular, $\sigma = 0$ corresponds to the Viana-Bray model.[26] For $1/2 < \sigma \leq 2/3$ the model describes a mean-field, long-range spin glass,[17] corresponding to a short-range model with a space dimension above the upper critical dimension, i.e., $d \geq d_{\rm u} = 6$.[27,28] For $2/3 < \sigma \leq 1$ the model has nonmean-field critical behavior with a finite transition temperature T_c, while for $\sigma \geq 1$, the transition temperature is zero.[17] The value of σ in the long-range one-dimensional model corresponds roughly to an effective space dimension d in a short-range model via the relation[18–20]

$$d = \frac{2 - \eta(d)}{2\sigma - 1} \,, \tag{4}$$

where $\eta(d)$ is the critical exponent η for the short-range model, which is zero in the mean-field regime. Here we are interested in values of σ that correspond to three- (3D) and four-dimensional (4D) short-range systems. Because $\eta(d = 3) = -0.384(9)$,[29] three dimensions corresponds to $\sigma_{d=3} \simeq 0.896$, and since $\eta(d = 4) = -0.275(25)$,[30] four space dimensions corresponds to $\sigma_{d=4} \simeq 0.784$.

B. Observables

To determine whether a spin-glass state exists in a magnetic field, we study the wave-vector-dependent spin-glass susceptibility defined by

$$\chi_{\rm SG}(k) = \frac{1}{L} \sum_{i,j} \left[\Big(\langle S_i S_j \rangle_T - \langle S_i \rangle_T \langle S_j \rangle_T \Big)^2 \right]_{\rm av} e^{ik\,(i-j)}, \tag{5}$$

where $\langle \cdots \rangle_T$ denotes a thermal average and $[\cdots]_{\rm av}$ an average over the disorder. Each thermal average is obtained from a separate spin replica, i.e., we simulate four copies with the same disorder but different Markov chains at each temperature. As discussed in Sec. I, $\chi_{\rm SG}(k)$ is an appropriate quantity to study because $\chi_{\rm SG} \equiv \chi_{\rm SG}(k = 0)$ diverges on the AT line.

It is also convenient to extract from the spin-glass susceptibility a correlation length, which is usually defined by[14,18,31,32]

$$\xi_L = \frac{1}{2\sin(k_1/2)} \left[\frac{\chi_{\rm SG}(0)}{\chi_{\rm SG}(k_1)} - 1 \right]^{1/(2\sigma-1)} , \tag{6}$$

where $k_1 = 2\pi/L$ is the smallest nonzero wave vector. Because we work in the nonmean-field regime, standard finite-size-scaling (FSS) applies, i.e.,

$$\xi_L/L = \mathcal{X}[L^{1/\nu}(T - T_c)] \,. \tag{7}$$

The importance of ξ_L/L is that it is dimensionless. As such, data for ξ_L/L for different system sizes L cross at the transition temperature $T = T_c$ if corrections to FSS are unimportant [see, for example, Fig. 1(a)]. This is a particularly convenient way to locate T_c.

For the one-dimensional model the critical exponent $\eta_{\rm LR}$ satisfies the *exact* relation $2 - \eta_{\rm LR} = 2\sigma - 1$, so it is also convenient to study the finite-size scaling of a second scale-invariant quantity, namely

$$\chi_{\rm SG}/L^{2-\eta_{\rm LR}} = \chi_{\rm SG}/L^{2\sigma-1} = \mathcal{C}[L^{1/\nu}(T - T_c)] \,. \tag{8}$$

Again, if FSS applies without corrections, data for $\chi_{\rm SG}/L^{2\sigma-1}$ for different system sizes cross at T_c.

Both the correlation length in Eq. (7) and the spin-glass susceptibility in Eq. (8) involve $k = 0$ fluctuations. Recently, Refs. 22, 23 and 34 have argued that one should avoid data at $k = 0$ for spin glasses in the presence of a magnetic field on the grounds that there are large corrections to FSS. We discuss this in detail below and for now just present the new proposed quantities to be measured[22,23,34] that avoid $k = 0$ fluctuations. We shall use the term "modified" FSS scaling analysis to denote the use of these quantities. Below we compare the results of this modified analysis with results obtained from Eqs. (7) and (8), which we denote the "standard" FSS approach.

At long wavelength one expects

$$\chi_{\rm SG}(k)^{-1} = \chi_{\rm SG}(0)^{-1} + By + Cy^2 \tag{9}$$

with $y = k^{2\sigma-1}$, which is the generalization of the Ornstein-Zernicke equation to long-range interactions, so one can calculate $\chi_{\rm SG}(0)^{-1}$ *indirectly* by fitting data for nonzero k to this form. For $L \to \infty$, this extrapolated value, $\chi_{\rm SG}(k \to 0)^{-1}$, vanishes at and below the transition temperature. Interestingly, one finds[22,23] that the extrapolated value goes through zero even for a finite system, at a temperature $T^\star(L)$ which tends to T_c for $L \to \infty$. This means $T_c = \lim_{L\to\infty} T^\star(L)$. We find quite strong corrections to the asymptotic result (as found also for the Sherrington-Kirkpatrick model in Ref. 35), so we include the leading correction to scaling by fitting the data to

$$T^\star(L) = T_c + \frac{A}{L^\lambda}, \tag{10}$$

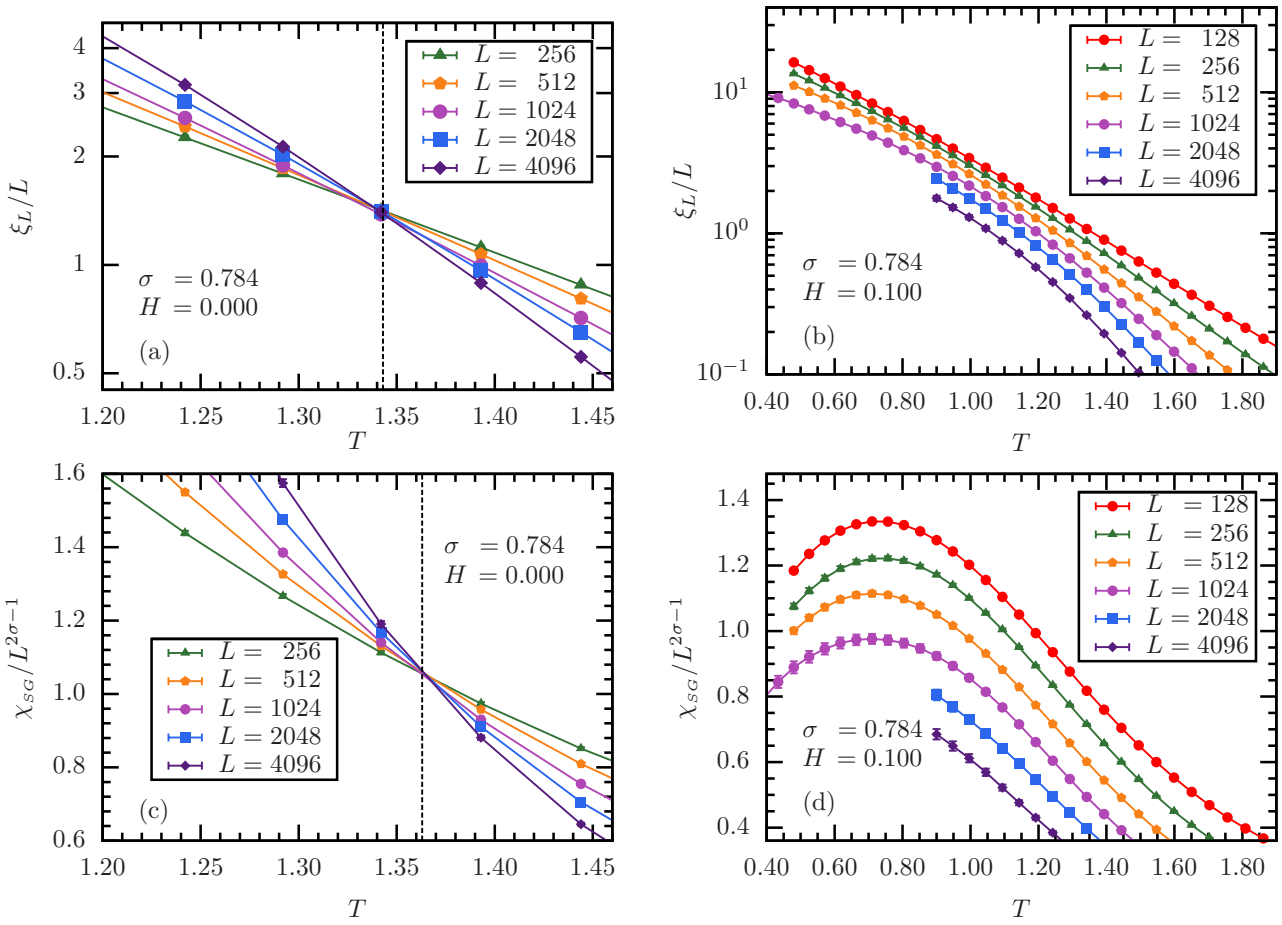

FIG. 1: (Color online) Data used in a standard FSS for $\sigma = 0.784$, which is a proxy for four dimensions. The left column is for $H = 0$, the right column for $H = 0.1$. The top row shows the finite-size correlation length divided by L as a function of temperature T for different system sizes. The bottom row shows results for the scale-invariant spin-glass susceptibility, $\chi_{\rm SG}/L^{2\sigma-1}$. The intersections seen in the left-hand column indicate a transition in zero field. The intersection temperatures (shown by the dashed vertical line) are $T_c \simeq 1.34$ from ξ_L/L data in part (a), and $T_c \simeq 1.36$ from $\chi_{\rm SG}/L^{2\sigma-1}$ data in part (c). The small difference is likely due to sensitive corrections to scaling in the susceptibility (see Ref. 33 for details). By contrast, the lack of intersections in the right-hand column indicates no transition in a magnetic field.

where λ is a correction to scaling exponent and A is the amplitude of the correction.

This method requires several nonzero wavevectors and so is particularly suitable for one-dimensional models as studied here, because one can simulate very large *linear* sizes for these. For a *short-range* model in 4D, where the number of wavevectors is more limited, Ref. 34 propose another quantity. To motivate this quantity, we note as stated above, that ξ_L/L is particularly useful because it is dimensionless. From Eq. (6) we see that the crucial quantity is the ratio $\chi_{\rm SG}(0)/\chi_{\rm SG}(k_1)$ which is also dimensionless. Massaging this quantity to obtain another dimensionless quantity ξ_L/L according to Eq. (6) is actually not essential. Therefore, a related quantity which does not involve $k = 0$ can be defined via

$$R_{12} = \frac{\chi_{\rm SG}(k_1)}{\chi_{\rm SG}(k_2)}\,, \qquad (11)$$

where $k_2 = 4\pi/L$ is the second smallest nonzero wave vector. Because it is dimensionless, R_{12} has the same FSS form as ξ_L/L shown in Eq. (7). Consequently, curves of R_{12} for different system sizes L should intersect at T_c if corrections to FSS are unimportant.

C. Numerical Details

The simulations are done using the parallel tempering (exchange) Monte Carlo method.[36,37] Simulation parameters are listed in Table I. Equilibration is tested using the method developed in Ref. 18 [Eq. (8)]: The energy per spin is computed directly, as well as as a function of a spin correlator. Both have to agree if a system is in thermal equilibrium. Starting from a random configuration, the directly-computed energy is typically overestimated, while the energy computed from the correlator is underestimated. Only when both agree (on average) is the system in thermal equilibrium. We thus perform a logarithmic binning of the data and requiring that both the energy per spin and the energy computer from the corre-

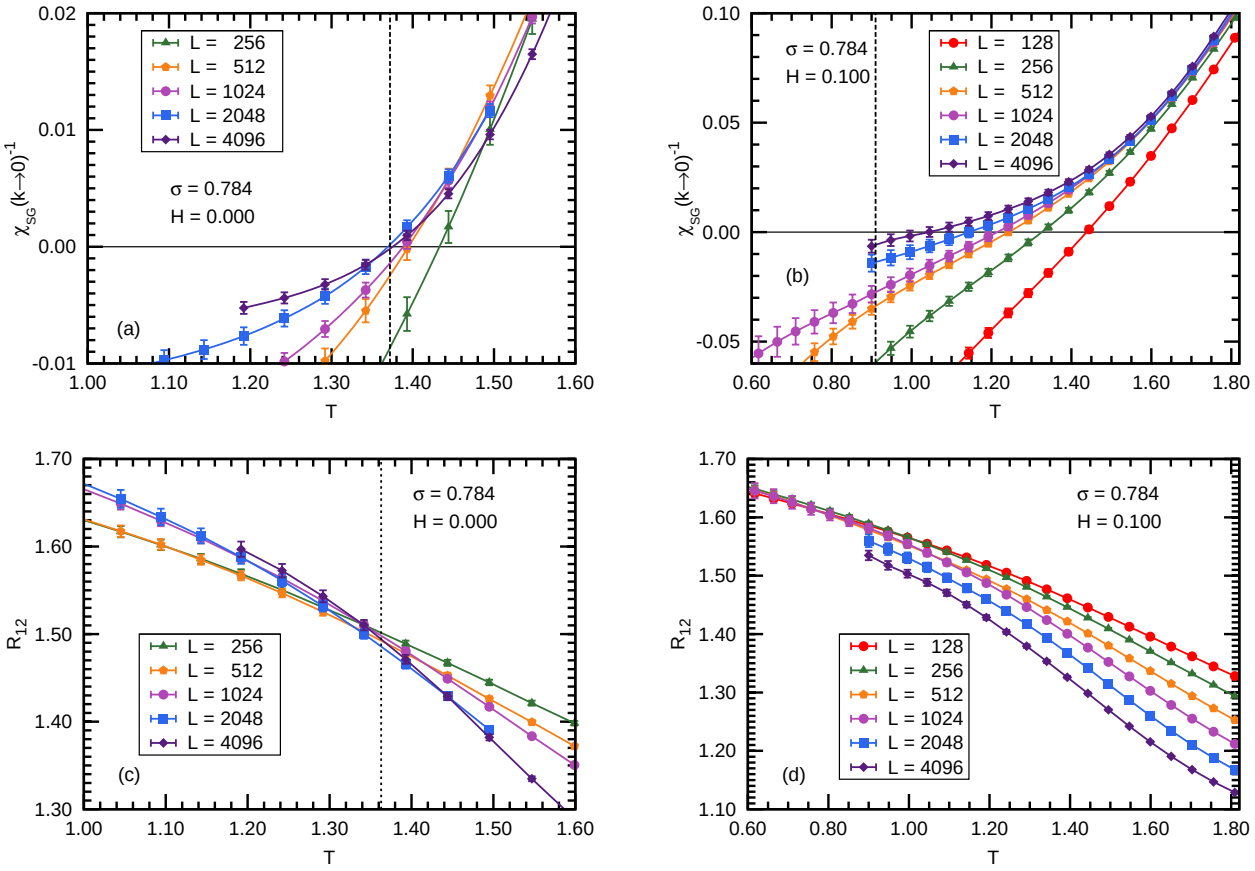

FIG. 2: (Color online) Data used in the modified FSS analysis for $\sigma = 0.784$. As in Fig. 1, the left column is for $H = 0$ and the right column for $H = 0.1$. The top row shows the inverse spin-glass susceptibility $\chi_{\rm SG}(k \to 0)^{-1}$ extrapolated from results for $k \neq 0$. The bottom row shows data for the dimensionless ratio R_{12} defined in Eq. (11). The dashed line for $\chi_{\rm SG}(k \to 0)^{-1}$ [top row, panels (a) and (b)] indicates the extrapolated transition temperature T_c determined from the fits in Fig. 3. The R_{12} data for $H = 0$ [panel (c)] show intersections but the trend of intersection temperatures is not smooth for this range of sizes. The dotted vertical line shows the transition temperature estimated from the intersections of $\chi_{\rm SG}/L^{2\sigma-1}$ in Fig. 1 ($T_c = 1.36$) and so is just a guide to the eye. The R_{12} data for $H = 0.1$ [panel (d)] show no sign of a transition in the range of temperatures studied.

lator agree for at least the last two logarithmic bins. The reason we wait for two additional logarithmic bins is because the equality only holds on average. By being more conservative with the equilibration times we ensure that the bulk of the samples are in thermal equilibrium.[38] In addition, we verify that all other observables are independent of Monte Carlo time for at least these last two bins.

III. RESULTS

A. $\sigma = 0.784$ (four space dimensions)

When $\sigma = 0.784$ the one-dimensional model is a proxy for a short-range model in four space dimensions. Data for ξ_L/L and $\chi_{\rm SG}/L^{2\sigma-1}$, used within the standard FSS, are shown in Fig. 1 for $H = 0$ (left column) and $H = 0.1$ (right column). The zero-field data for the scaled $\chi_{\rm SG}$ in Fig. 1(c) show clear intersections indicating a transition at $T_c \simeq 1.36$, while the data for ξ_L/L in Fig. 1(a) show clear intersections at $T_c \simeq 1.34$. This (small) difference is presumably due to corrections to scaling. Because there is no doubt that there is a zero-field transition for the models studied in this paper (see e.g., Ref. 20) we have not carried out a precise estimate of the value of T_c in zero field.

In contrast to the zero field data, the data in a field of $H = 0.1$, Figs. 1(b) and 1(d), show no intersections indicating the absence of a transition, at least for this range of temperatures and field.

Data for the extrapolated value of $\chi_{\rm SG}(k \to 0)^{-1}$ fitted according to Eq. (9) and R_{12} defined via Eq. (11) are shown in Fig. 2 and used in the modified FSS. The zero-field data for R_{12} in Fig. 2(c) show intersections but the intersection temperatures do not vary monotonically for this range of sizes. The dotted vertical line in Fig. 2(c) corresponds to T_c from the scaled $\chi_{\rm SG}$ data in Fig. (1)(c), and so is only a guide to the eye. The data for R_{12} in a field ($H = 0.1$) in Fig. 2(d) have no intersections, i.e., no

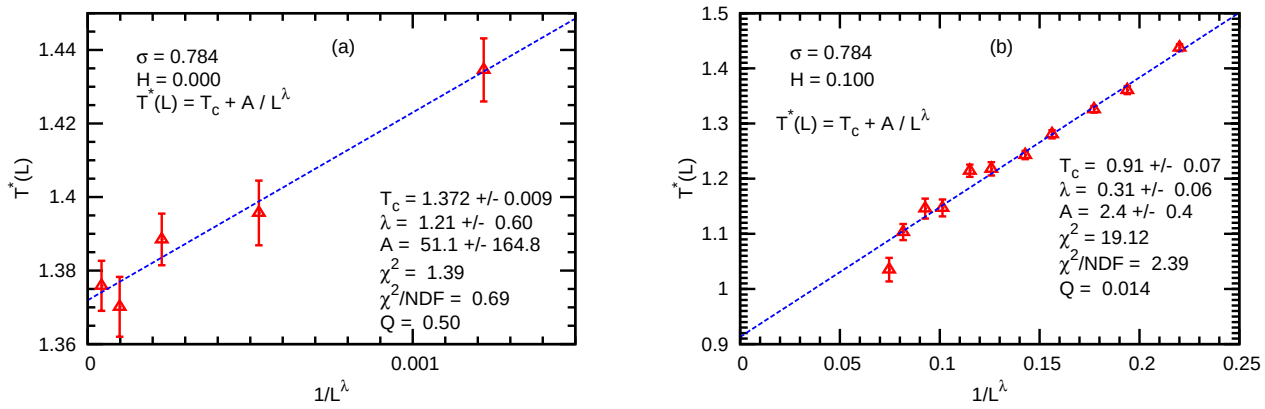

FIG. 3: (Color online) Values of $T^\star(L)$, the temperature where $\chi_{\rm SG}(k\to 0)^{-1}$ goes through zero, for different system sizes for $H=0$ (left) and $H=0.1$ (right) for $\sigma=0.784$. The data are fitted to Eq. (10) with T_c, A and λ as adjustable parameters. In both cases a finite value of T_c (the intercept) is found. For $H=0$ the goodness of fit parameter[39,40] Q is not very small indicating a satisfactory fit. For $H=0.1$ the value of Q is smaller because the point for the largest size is well below the fit.

transition is visible for the range of temperatures studied.

For each system size, the temperature where the data for $\chi_{\rm SG}(k\to 0)^{-1}$ shown in Figs. 2(a) and 2(b) goes through zero is referred to as $T^\star(L)$. This value is obtained by fitting the data to a cubic polynomial (using the seven data points nearest to zero), and error bars are obtained from a bootstrap analysis. The results are shown in Fig. 3. The thermodynamic transition temperature T_c is then given by $\lim_{L\to\infty} T^\star(L)$, which we estimate by fitting to Eq. (10). The fits, obtained by adjusting T_c, A and λ, are shown in the figures (dashed lines). The data indicate a finite value of T_c both in a field and in zero field. The central values for T_c are shown by the dashed vertical lines in Figs. 2(a) and 2(b). The value of $\chi^2/N_{\rm DOF}$ where $N_{\rm DOF}$ is the number of degrees of freedom, and the goodness of fit parameter[39,40] Q, indicate a good fit in the case of $H=0$ ($Q=0.50$). For $H=0.1$ the value of Q is smaller ($Q=0.014$) because the point for the largest size is well below the fit.

Our analysis to ascertain whether there is a finite T_c includes four sets of data: ξ_L/L, $\chi_{\rm SG}/L^{2\sigma-1}$, $\chi_{\rm SG}(k\to 0)^{-1}$ and R_{12}. In zero field they all clearly show a finite transition temperature, in agreement with the work of Baños *et al.*[20] who studied almost the same model. However, in a field of $H=0.1$ there is an inconsistency: Three of the four measures (ξ_L/L, $\chi_{\rm SG}/L^{2\sigma-1}$ and R_{12}) show no sign of a transition. In contrast, the value of T_c from results for $\chi_{\rm SG}(k\to 0)^{-1}$ does appear to be nonzero ($T_c=0.91\pm 0.07$), see Fig. 3(b). We note, however, that the error bar is large and the last data point being below the fit may possibly indicate a downward trend at larger sizes.

This discrepancy highlights the need to better understand FSS in spin glasses in a magnetic field. We shall come back to this question in Sec. IV. However, already we note that because the $\chi_{\rm SG}(k\to 0)^{-1}$ data are the *only* indicator for a finite T_c in a field, we feel we should view results for this quantity with caution.

B. $\sigma = 0.896$ (three space dimensions)

The one-dimensional long-range model with $\sigma=0.896$ is a proxy for a short-range spin glass in three space dimensions. The data used in the standard FSS analysis are shown in Fig. 4. Again, the left column is for $H=0$ and the right column is for $H=0.1$. The zero field results for the scaled $\chi_{\rm SG}$ in Fig. 4(c) show a clear transition. The zero field data for ξ_L/L in Fig. 4(a) are less clear cut because there is little splaying of the data at low temperatures. However, the temperature where the data merge for two neighboring sizes *increases* as the system size increases. Similar results were obtained by Baños *et al.*[20] for almost the same model, although they were able to study size of up to $L=8192$ which do show a clear intersection with the data for $L=4096$ (see Fig. 15 in their paper). Performing a detailed FSS analysis, Baños *et al.*[20] showed that all their data *are* consistent with a finite value of T_c. Because our data for ξ_L/L do not in itself convincingly locate the transition temperature, the dotted line in Fig. 4(a) shows (as a guide to the eye) the location of T_c as determined from the scaled $\chi_{\rm SG}$ data in Fig. 4(c).

In a field, the data for ξ_L/L in Fig. 4(b) and the scaled spin-glass susceptibility in Fig. 4(d) show no intersections and hence indicate that there is no transition for this range of temperature and field.

Data for the modified FSS analysis are shown in Fig. 5. The results for R_{12} are shown in the bottom row. In zero field [see Fig. 5(c)] there are clear intersections although these do not vary monotonically for the range of sizes studied. However, the data are consistent with the value $T_c\simeq 0.795$ obtained from the scaled $\chi_{\rm SG}$ data in Fig. 4(c), and this value is indicated as a guide to the eye by the dotted vertical line in Fig. 5(c). The data for R_{12} in a field $H=0.1$ [Fig. 5(d)] do not show clear evidence for a transition in the range of temperatures studied.

The top row of Fig. 5 shows results for $\chi_{\rm SG}(k\to 0)^{-1}$.

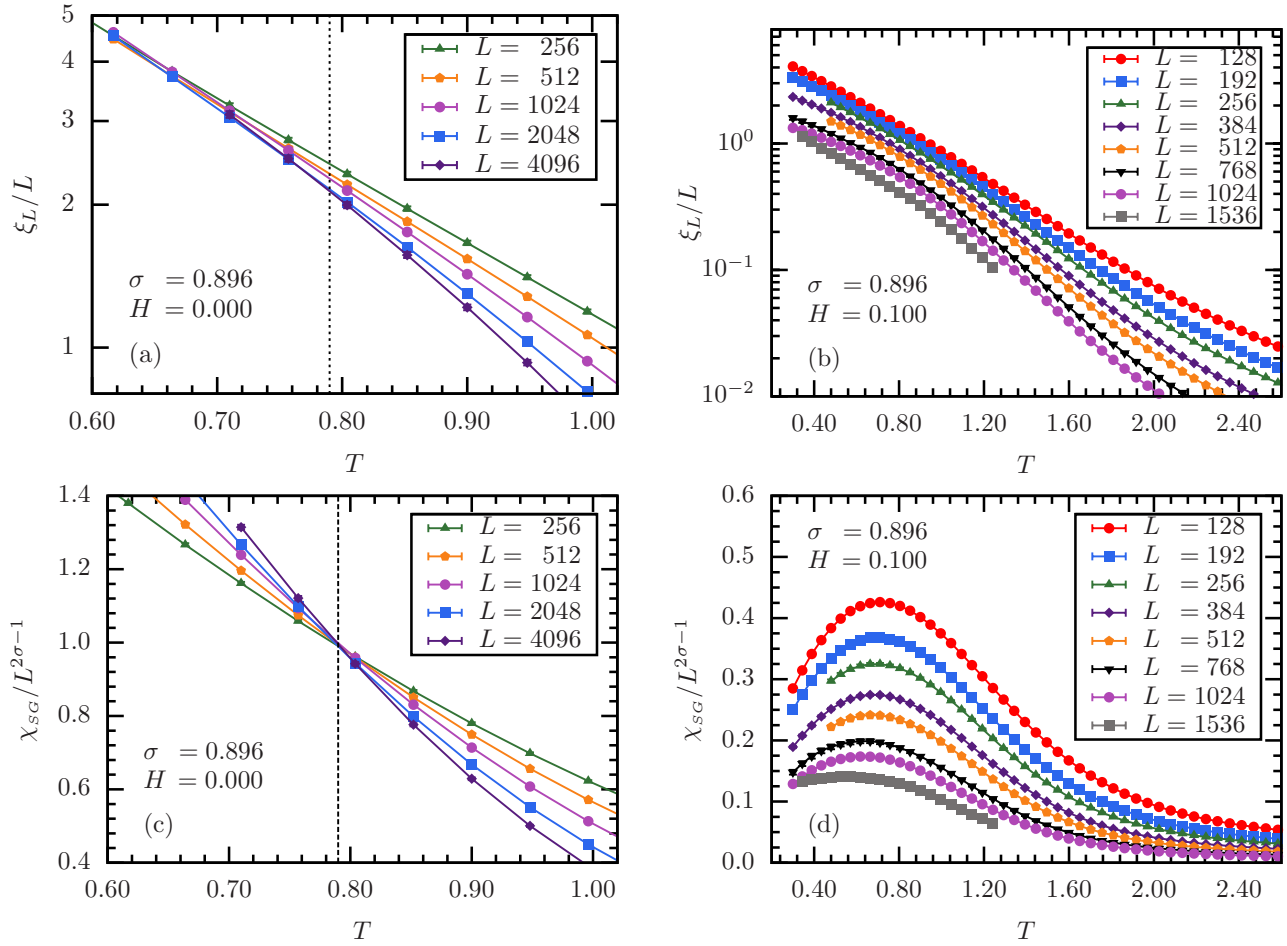

FIG. 4: (Color online) Data used in the standard FSS for $\sigma = 0.896$, which is a proxy for three space dimensions. The left column is for $H = 0$, the right column for $H = 0.1$. The top row shows the finite-size correlation length divided by L as a function of T for different system sizes. The bottom row shows results for the scale-invariant spin-glass susceptibility, $\chi_{\rm SG}/L^{2\sigma-1}$. The intersections in the data for $\chi_{\rm SG}/L^{2\sigma-1}$ for $H = 0$ [panel (c)] indicate a transition at $T_c \simeq 0.795$, which is shown by a dashed vertical line. The zero field results for ξ_L/L [panel (a)] show stronger finite-size effects and the evidence for intersections is not so clear. The same result was found recently by Baños *et al.*[20] who were able to study somewhat larger sizes for almost the same model. Their FSS analysis of all their data supports a zero-field transition. In panel (a) the dotted vertical line indicates the transition temperature found for the data in panel (c) and so is just a guide to the eye. The data in panel (a) are consistent with intersections tending to this value for $L \to \infty$. By contrast, the lack of intersections in the right-hand column indicates no transition in a magnetic field.

The temperatures where $\chi_{\rm SG}(k \to 0)^{-1} = 0$ are plotted and fitted according to Eq. (10) in Fig. 6. The values of Q, 0.37 for $H = 0$ and 0.91 for $H = 0.1$, indicate a good fit. For $H = 0$ the result is $T_c = 0.81 \pm 0.03$ and the central value is indicated by the dashed vertical line in Fig. 5(a). This value is consistent with the value 0.795 from the data for the scaled $\chi_{\rm SG}$ in Fig. 4(c). For $H = 0.1$, the values of $T^\star(L)$ shown in Fig. 6(b) have a very strong size dependence. The figure also shows the values of the parameters obtained by fitting the data to (10). In particular, we find $T_c = -0.37 \pm 1.15$, indicating that the optimal T_c is negative but the error bar is very large. This large error bar requires more discussion, which we now give.

First we note that a log-log plot of the data in Fig. 7 indicates that the data are compatible with $T_c = 0$. In addition, we perform the following analysis: For each system size we construct 200 bootstrap data sets and estimate $T^\star(L)$ for each of them. There is a huge scatter in the estimates from the largest size $L = 1536$. Thus we ignore this size in the analysis. For $L = 784$, 9 of the 200 bootstrap data sets do not yield a temperature where $\chi_{\rm SG}(k \to 0)^{-1}$ vanishes. Hence we consider 191 bootstrap data sets and fit each of them according to Eq. (10).

Figure 8 shows the resulting cumulative distribution of transition temperatures, i.e., the probability that the transition temperature is less than the stated value. We find that 34 of the 191 data sets do not have a minimum in χ^2; rather, considering χ^2 as a function of T_c while optimizing with respect to the other fit parameters, χ^2 decreases monotonically as $T_c \to -\infty$ while $\lambda \to 0$ in this

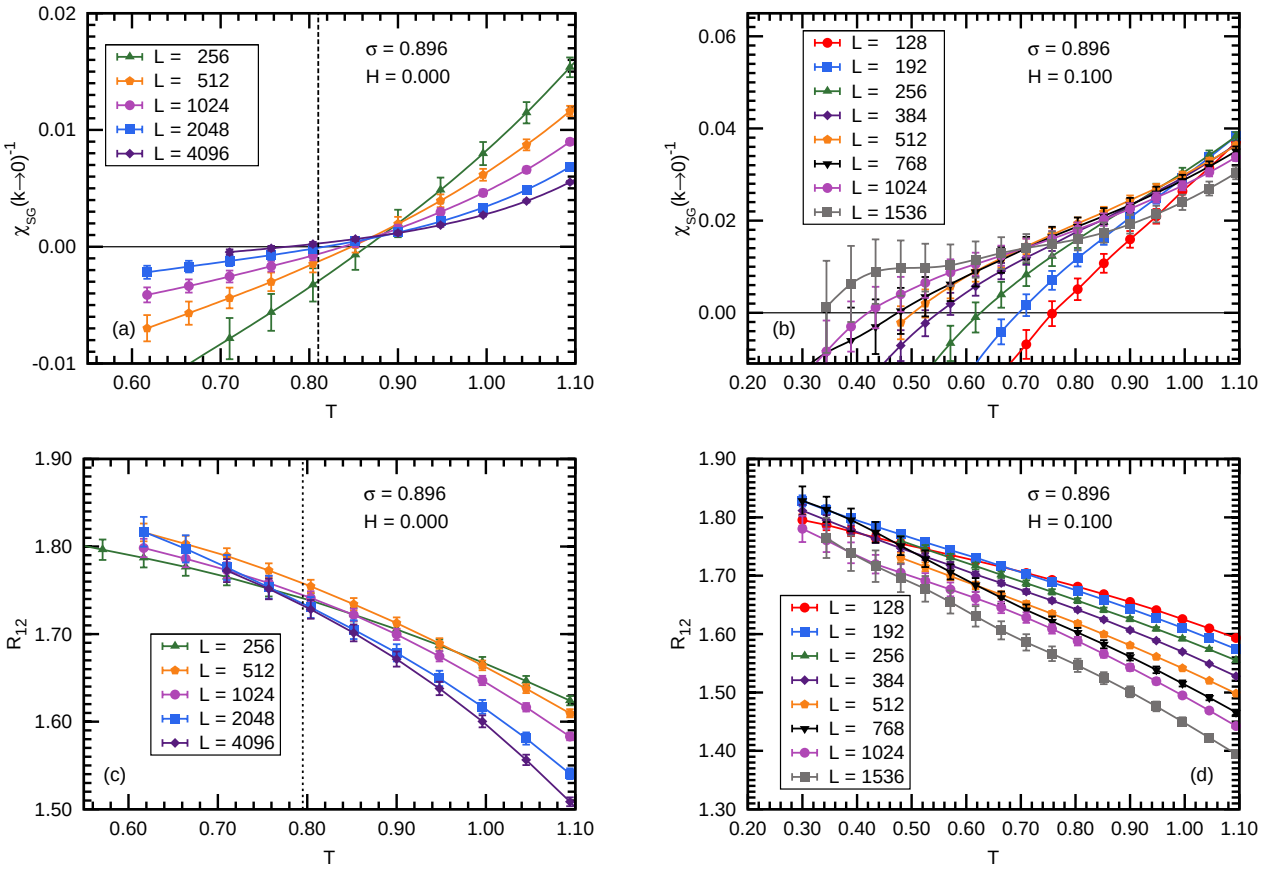

FIG. 5: (Color online) Data used in the modified FSS analysis for $\sigma = 0.896$. As in Fig. 4, the left column is for $H = 0$ and the right column for $H = 0.1$. The top row shows the inverse spin-glass susceptibility $\chi_{\rm SG}(k \to 0)$ extrapolated from results for $k \neq 0$. The bottom row shows data for the dimensionless ratio R_{12} defined in Eq. (11). The dashed vertical line in panel (a) marks the value for T_c obtained by extrapolating the data for $T^\star(L)$ [where $\chi_{\rm SG}(k \to 0)^{-1}$ vanishes] according to Eq. (10), see Fig. 6. The result is $T_c = 0.81(3)$ in agreement with the value of 0.795 from the intersections of the scaled $\chi_{\rm SG}$ in Fig. 4(c). The data for R_{12} in zero field in panel (c) show intersections, although the intersection temperatures do not vary smoothly. The dotted vertical line shows T_c obtained from the scaled $\chi_{\rm SG}$ and is just a guide to the eye. The results for R_{12} for $H = 0.1$ in panel (d) do not provide clear evidence for a transition.

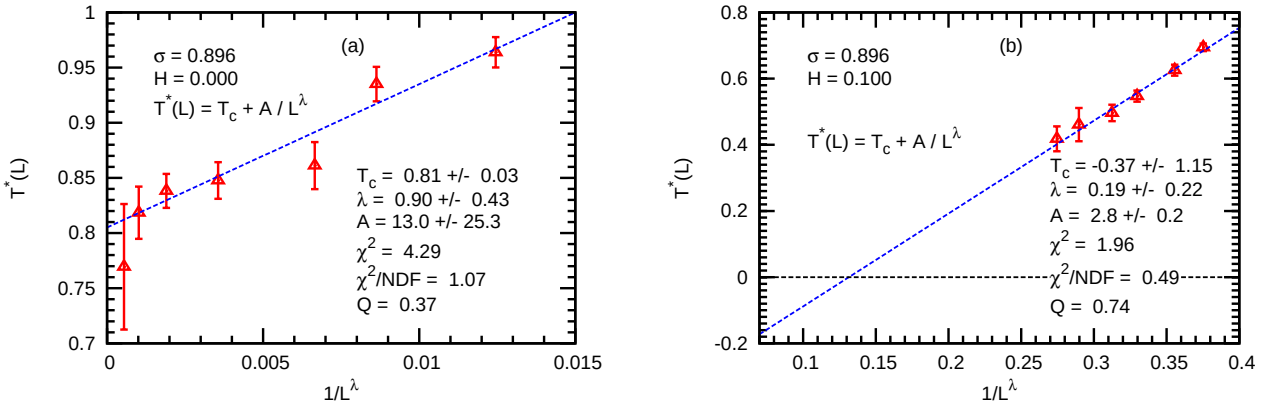

FIG. 6: (Color online) Values of $T^\star(L)$, the temperature where $\chi_{\rm SG}(k \to 0)^{-1}$ goes through zero, for different system sizes for $H = 0$ (left) and $H = 0.1$ (right) for $\sigma = 0.896$. The data are fitted to Eq. (10) with T_c, A and λ as adjustable parameters. The error bars on the parameters in the fit to the $H = 0.1$ data are very large (this is discussed in the text and in the caption to Fig. 8). Note already, though, that the $H = 0.1$ data are consistent with $T_c = 0$. The goodness of fit parameter[40] indicates a satisfactory fit in both cases.

limit. The estimate of T_c from the global fit ($T_c = -0.37$, indicated by the dashed vertical line) agrees well with the

TABLE I: Parameters of the simulations for different field strengths H and exponents σ. $N_{\rm sa}$ is the number of samples, $N_{\rm sw}$ is the total number of Monte Carlo sweeps, $T_{\rm min}$ is the lowest temperature simulated, and N_T is the number of temperatures used in the parallel tempering method for each system size L. The last column shows the parameter $\mathcal{A}$ in Eq. (2) for $z_{\rm av} = 6$ neighbors.

σ	H	L	$N_{\rm sa}$	$N_{\rm sw}$	$T_{\rm min}$	N_T	$\mathcal{A}$
0.784	0.0	256	10179	20	0.617	43	1.86026
0.784	0.0	512	10068	20	0.617	43	1.82182
0.784	0.0	1024	10240	20	0.617	43	1.79706
0.784	0.0	2048	4810	20	0.710	17	1.78084
0.784	0.0	4096	4400	20	1.192	17	1.77010
0.784	0.1	128	37484	20	0.480	46	1.92172
0.784	0.1	192	30150	20	0.480	46	1.88220
0.784	0.1	256	37494	20	0.480	46	1.86026
0.784	0.1	384	27970	20	0.480	46	1.83571
0.784	0.1	512	32856	20	0.480	46	1.82182
0.784	0.1	768	9988	20	0.344	49	1.80607
0.784	0.1	1024	9995	21	0.344	49	1.79706
0.784	0.1	1536	7163	20	0.900	28	1.78676
0.784	0.1	2048	5116	20	0.900	28	1.78084
0.784	0.1	3072	4306	20	0.900	28	1.77403
0.784	0.1	4096	6592	20	0.900	28	1.77010
0.896	0.0	128	14800	20	0.617	43	2.78392
0.896	0.0	192	10770	20	0.617	43	2.76125
0.896	0.0	256	9830	20	0.617	43	2.74955
0.896	0.0	512	11632	20	0.617	43	2.73087
0.896	0.0	1024	11052	20	0.617	43	2.72041
0.896	0.0	2048	4345	20	0.617	43	2.71446
0.896	0.0	4096	5230	20	0.710	17	2.71105
0.896	0.1	128	45000	20	0.300	50	2.78392
0.896	0.1	256	32333	20	0.480	46	2.74955
0.896	0.1	384	45000	20	0.300	50	2.73732
0.896	0.1	512	28603	20	0.480	46	2.73087
0.896	0.1	768	8036	21	0.480	46	2.72405
0.896	0.1	1024	9285	21	0.300	50	2.72041

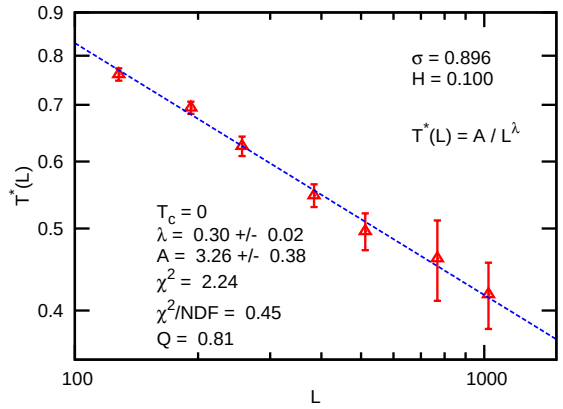

FIG. 7: (Color online) Log-log plot of the data for $T^\star(L)$ for $\sigma = 0.896$ and $H = 0.1$ assuming $T_c = 0$. The fit works very well according to the goodness of fit parameter Q which is 0.81.

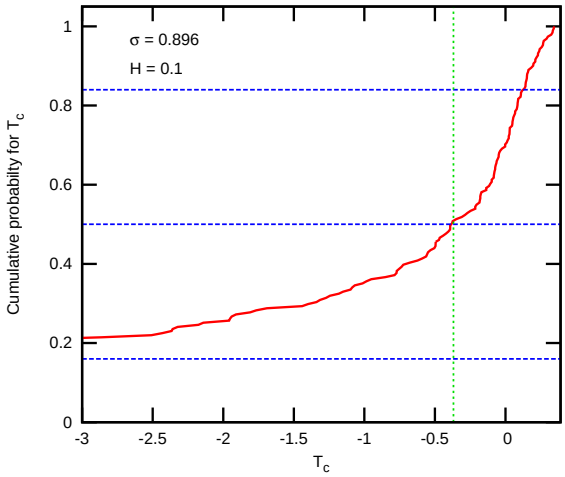

FIG. 8: (Color online) Cumulative distribution of the transition temperature T_c obtained from a bootstrap analysis of the data for $\sigma = 0.896$ and $H = 0.1$. The estimate of T_c from the global fit ($T_c = -0.37$, indicated by the dashed vertical line) agrees well with the median (50 percentile) of the bootstrap estimates which is indicated by a horizontal dashed line. Also indicated by horizontal dashed lines are the 16 and 84 percentiles which would correspond to one standard deviation if the distribution of T_c's were Gaussian, which is clearly not the case. Only 30% of the bootstrap fits have a positive T_c.

median (50 percentile) of the bootstrap estimates. The median is indicated by a horizontal dashed line. Also indicated by horizontal dashed lines are the 16 and 84 percentiles which would correspond to one standard deviation if the distribution of T_c's were Gaussian, which is clearly not the case here. Only 30% of the bootstrap fits have a positive T_c. We therefore conclude that a positive T_c is somewhat unlikely, but cannot be completely excluded by the data for $T^\star(L)$.

To conclude this subsection, *all* data are consistent with there being no AT line at $H = 0.1$ for $\sigma = 0.896$. The results for $T^\star(L)$ obtained from the vanishing of $\chi_{\rm SG}(k \to 0)^{-1}$ do not exclude a finite T_c, but this possibility does not seem to be supported by the rest of the data.

IV. CONCLUSIONS

We have presented results of simulations of one-dimensional spin-glass models in a magnetic field which are proxies for short-range models in three and four space dimensions. We have analyzed the results using both a traditional FSS approach (which uses $k = 0$ data) and a recently-proposed modified FSS approach which uses only $k > 0$ data.

For the model which is a proxy for a 3D system, all our results are consistent with there being no transition in a magnetic field, at least for the range of fields and temperatures that we can study. The results for $T^\star(L)$, obtained from the modified FSS analysis, are just compatible with a finite T_c but the other data are only compatible with the absence of a transition, at least assuming that the

data are in the asymptotic scaling region.

For the model which is a proxy for a 4D system, three out of the four sets of data indicate the absence of a transition in a field (ξ_L/L, $\chi_{\rm SG}/L^{2\sigma-1}$, and R_{12}), while that for $T^\star(L)$ gives a satisfactory fit indicating $T_c > 0$. This contradiction indicates that at least some of the data cannot be in the asymptotic scaling region.

It is therefore crucial to understand whether it is better to use $k = 0$ data in the analysis as in the standard approach, or to exclude that data as in the modified approach.[22,23,34] References 22, 23, and 34 argue that the $k = 0$ data have strong corrections to FSS. On the other hand, the divergence occurs at $k = 0$ and normally one uses divergent quantities in FSS because these should show the asymptotic FSS behavior for the smaller system sizes. It should also be noted that Ref. 16 found good agreement for the location of the AT line for the spin glass on a random graph, i.e., the Viana-Bray model (which corresponds to the $\sigma = 0$ limit of the present model), using the scaled $\chi_{\rm SG}$, i.e., the $k = 0$ fluctuations.

Finally, an alternate interpretation of the results can be done using droplet scaling arguments.[4–7] The size $\xi_{\rm D}$ of the droplets within this picture can be estimated by equating the domain-wall energy required to create them, $\sim J\xi_{\rm D}^{\theta}$, to the energy which can be gained from flipping a droplet of size $\xi_{\rm D}$ in the field, $\sim H\xi_{\rm D}^{d/2}$, where d is the space dimension. For the long-range models studied here, $\theta = 1 - \sigma$.[17] Thus the droplet size is of order 3320 for $\sigma = 0.784$ and is of order 335 at $\sigma = 0.896$, when $H/J = 0.1$, the ratio used in this study. We have only one data point, that for $L = 4096$ in Fig. 6(b), greater than 3320. Interestingly, it is the data points at the smaller values of L which point to a finite value of T_c. The last point at system size 4096 lies well below the fitted curve. This suggests that had we been able to obtain data for a range of system sizes significantly greater than 4096, it might have been possible to obtain results in the analogue of four dimensions like that displayed in Fig. 7 for the analogue of three dimensions, where the last five data points are all greater than the estimated droplet size there of 335 and the extrapolated value of T_c is zero.

Ideally one would determine which set of data is in the asymptotic scaling regime by simulating larger system sizes. However, because the present study involved a rather substantial amount of CPU time, this is not feasible for us at present. Based on the data shown, the balance of the evidence is that there is no AT line in the one-dimensional models which are proxies for three and four dimensional short-range spin glasses. However, a deeper insight into corrections to FSS in spin glasses is needed to confirm this conclusion.

Acknowledgments

H.G.K. acknowledges support from the Swiss National Science Foundation (Grant No. PP002-114713) and the National Science Foundation (Grant No. DMR-1151387). We would like to thank the Texas Advanced Computing Center (TACC) at The University of Texas at Austin for providing HPC resources (ranger and lonestar clusters), ETH Zurich for CPU time on the brutus cluster, and Texas A&M University for access to their eos and lonestar clusters. A.P.Y acknowledges support from the NSF under Grants DMR-0906366 and DMR-1207036.

[1] G. Parisi, *The order parameter for spin glasses: a function on the interval* 0–1, J. Phys. A **13**, 1101 (1980).

[2] D. Sherrington and S. Kirkpatrick, *Solvable model of a spin glass*, Phys. Rev. Lett. **35**, 1792 (1975).

[3] J. R. L. de Almeida and D. J. Thouless, *Stability of the Sherrington-Kirkpatrick solution of a spin glass model*, J. Phys. A **11**, 983 (1978).

[4] D. S. Fisher and D. A. Huse, *Absence of many states in realistic spin glasses*, J. Phys. A **20**, L1005 (1987).

[5] D. S. Fisher and D. A. Huse, *Equilibrium behavior of the spin-glass ordered phase*, Phys. Rev. B **38**, 386 (1988).

[6] A. J. Bray and M. A. Moore, *Scaling theory of the ordered phase of spin glasses*, in *Heidelberg Colloquium on Glassy Dynamics and Optimization*, edited by L. Van Hemmen and I. Morgenstern (Springer, New York, 1986), p. 121.

[7] W. L. McMillan, *Scaling theory of Ising spin glasses*, J. Phys. A **17**, 3179 (1984).

[8] Unfortunately there is no *experimentally accessible* static quantity which diverges on the AT line. In zero field, the experimentally measurable non-linear susceptibility χ_{nl} is proportional to $\chi_{\rm SG}$ and both diverge at the *zero field* transition. However, in a magnetic field χ_{nl} does not couple to the divergent fluctuations in $\chi_{\rm SG}$. This is why the AT line was not seen in the original calculation of Sherrington and Kirkpatrick[2] but had to wait for the more detailed calculation of the fluctuations performed by de Almeida and Thouless[3].

[9] J. C. Ciria, G. Parisi, F. Ritort, and J. J. Ruiz-Lorenzo, *The de-Almeida-Thouless line in the four-dimensional Ising spin glass*, J. Phys. I France **3**, 2207 (1993).

[10] G. Migliorini and A. N. Berker, *Global random-field spin-glass phase diagrams in two and three dimensions*, Phys. Rev. B **57**, 426 (1998).

[11] E. Marinari, C. Naitza, and F. Zuliani, *Critical Behavior of the 4D Spin Glass in Magnetic Field*, J. Phys. A **31**, 6355 (1998).

[12] J. Houdayer and O. C. Martin, *Ising spin glasses in a magnetic field*, Phys. Rev. Lett. **82**, 4934 (1999).

[13] F. Krzakala, J. Houdayer, E. Marinari, O. C. Martin, and G. Parisi, *Zero-temperature responses of a 3D spin glass in a field*, Phys. Rev. Lett. **87**, 197204 (2001).

[14] A. P. Young and H. G. Katzgraber, *Absence of an Almeida-Thouless line in Three-Dimensional Spin Glasses*, Phys. Rev. Lett. **93**, 207203 (2004).

[15] H. Takayama and K. Hukushima, *Field-shift aging protocol on the 3D Ising spin-glass model: dynamical crossover between the spin-glass and paramagnetic states* (2004), (cond-mat/0307641).

[16] T. Jörg, H. G. Katzgraber, and F. Krzakala, *Behavior of Ising Spin Glasses in a Magnetic Field*, Phys. Rev. Lett. **100**, 197202 (2008).

[17] H. G. Katzgraber and A. P. Young, *Monte Carlo studies of the one-dimensional Ising spin glass with power-law interactions*, Phys. Rev. B **67**, 134410 (2003).

[18] H. G. Katzgraber, D. Larson, and A. P. Young, *Study of the de Almeida-Thouless line using power-law diluted one-dimensional Ising spin glasses*, Phys. Rev. Lett. **102**, 177205 (2009).

[19] D. Larson, H. G. Katzgraber, M. A. Moore, and A. P. Young, *Numerical studies of a one-dimensional 3-spin spin-glass model with long-range interactions*, Phys. Rev. B **81**, 064415 (2010).

[20] R. A. Baños, L. A. Fernandez, V. Martin-Mayor, and A. P. Young, *The correspondence between long-range and short-range spin glasses* (2012), (arXiv:1207.7014).

[21] L. Leuzzi, G. Parisi, F. Ricci-Tersenghi, and J. J. Ruiz-Lorenzo, *Diluted One-Dimensional Spin Glasses with Power Law Decaying Interactions*, Phys. Rev. Lett. **101**, 107203 (2008).

[22] L. Leuzzi, G. Parisi, F. Ricci-Tersenghi, and J. J. Ruiz-Lorenzo, *Ising Spin-Glass Transition in a Magnetic Field Outside the Limit of Validity of Mean-Field Theory*, Phys. Rev. Lett. **103**, 267201 (2009).

[23] L. Leuzzi, G. Parisi, F. Ricci-Tersenghi, and J. J. Ruiz-Lorenzo, *Bond diluted Levy spin-glass model and a new finite size scaling method to determine a phase transition*, Philos. Mag. **91**, 1917 (2011).

[24] T. Mori, *Instability of the mean-field states and generalization of phase separation in long-range interacting systems*, Phys. Rev. E **84**, 031128 (2011), (arXiv:1106.4920).

[25] M. Wittmann and A. P. Young, *Spin glasses in the nonextensive regime*, Phys. Rev. E **85**, 041104 (2012).

[26] L. Viana and A. J. Bray, *Phase diagrams for dilute spin glasses*, J. Phys. C **18**, 3037 (1985).

[27] A. B. Harris, T. C. Lubensky, and J.-H. Chen, *Critical Properties of Spin-Glasses*, Phys. Rev. Lett. **36**, 415 (1976).

[28] H. G. Katzgraber, *Spin glasses and algorithm benchmarks: A one-dimensional view*, J. Phys.: Conf. Ser. **95**, 012004 (2008).

[29] M. Hasenbusch, A. Pelissetto, and E. Vicari, *The critical behavior of 3D Ising glass models: universality and scaling corrections*, J. Stat. Mech. L02001 (2008).

[30] T. Jörg and H. G. Katzgraber, *Universality and universal finite-size scaling functions in four-dimensional Ising spin glasses*, Phys. Rev. B **77**, 214426 (2008).

[31] M. Palassini and S. Caracciolo, *Universal Finite-Size Scaling Functions in the 3D Ising Spin Glass*, Phys. Rev. Lett. **82**, 5128 (1999).

[32] H. G. Ballesteros, A. Cruz, L. A. Fernandez, V. Martin-Mayor, J. Pech, J. J. Ruiz-Lorenzo, A. Tarancon, P. Tellez, C. L. Ullod, and C. Ungil, *Critical behavior of the three-dimensional Ising spin glass*, Phys. Rev. B **62**, 14237 (2000).

[33] H. G. Katzgraber, M. Körner, and A. P. Young, *Universality in three-dimensional Ising spin glasses: A Monte Carlo study*, Phys. Rev. B **73**, 224432 (2006).

[34] R. A. Baños, A. Cruz, L. A. Fernandez, J. M. Gil-Narvion, A. Gordillo-Guerrero, M. Guidetti, D. Iñiguez, A. Maiorano, E. Marinari, V. Martin-Mayor, et al., *Thermodynamic glass transition in a spin glass without time-reversal symmetry*, Proc. Natl. Acad. Sci. USA **109**, 6452 (2012).

[35] A. Billoire and B. Coluzzi, *Magnetic field chaos in the SK model*, Phys. Rev. E **67**, 036108 (2003).

[36] C. Geyer, in *23rd Symposium on the Interface*, edited by E. M. Keramidas (Interface Foundation, Fairfax Station, 1991), p. 156.

[37] K. Hukushima and K. Nemoto, *Exchange Monte Carlo method and application to spin glass simulations*, J. Phys. Soc. Jpn. **65**, 1604 (1996).

[38] B. Yucesoy, J. Machta, and H. G. Katzgraber, *Correlations between the dynamics of parallel tempering and the free-*

energy landscape in spin glasses, Phys. Rev. E **87**, 012104 (2013).

[39] The goodness of fit parameter Q is the probability that, given the fit, the data could have the specified value for χ^2 or greater, assuming Gaussian noise, see for example Ref. [40].

[40] W. H. Press, S. A. Teukolsky, W. T. Vetterling, and B. P. Flannery, *Numerical Recipes in C* (Cambridge University Press, Cambridge, 1992).